STATIC AND FATIGUE ANALYSES OF RC BEAMS STRENGTHENED WITH CFR'P LAMINATES

Sherif El-Tawil, Member ASCE

Assistant Professor, Dept. of Civil and Env. Eng., U. of Central Florida, Orlando, FL 32816-2450 Ph. 407-823-3743, Fax 407-823-3315, Email: el-tawil@mail.ucf.edu

Cahit Ogunc
Graduate Research Assistant, Dept. of Civil and Env. Eng., U. of Central Florida, Orlando, FL 32816-2450

Ayman Okeil
Visiting Assistant Professor, Dept. of Civil and Env. Eng., U. of Central Florida, Orlando, FL 32816-2450

Mohsen Shahawy, Member ASCE
Chief Structural Analyst, Structural Research Center, FDOT, 2007 East Dirac Drive, Tallahassee, FL 32310.

ABSTRACT

Extensive testing has shown that externally bonded carbon fiber reinforced polymer (CFRP) laminates are particularly suited for improving the short term behavior of deficient reinforced concrete beams. Accelerated fatigue tests conducted to date confirm that fatigue response is also improved. This paper describes an analytical model for simulating the static response and accelerated fatigue behavior of reinforced concrete beams strengthened with CFRP laminates. Static and fatigue calculations are carried out using a fiber section model that accounts for the nonlinear time-dependent behavior of concrete, steel yielding, and rupture of CFRP laminates. Analysis results are compared to experimental data from two sets of accelerated fatigue tests on CFRP strengthened beams and show good agreement. Cyclic fatigue causes a time-dependent redistribution of stresses, which leads to a mild increase in steel and CFRP laminate stresses as fatigue life is exhausted. Based on the findings, design considerations are suggested for the repair and/or strengthening of reinforced concrete beams using CFRP laminates.

INTRODUCTION AND BACKGROUND

Worldwide concern about the deterioration of bridges has prompted extensive research efforts to find effective and economical rehabilitation means. One of the emerging technologies that has proven particularly suited for strengthening and stiffening reinforced concrete (RC) bridge girders is the use of externally bonded carbon fiber reinforced plastic (CFRP) material in " the form of plates or laminates. Plates are attached to the bottom surface of beams to provide additional tensile reinforcement. CFRP laminates (sheets) also provide extra tensile resistance and are attached to the bottom surface or wrapped around the stem of RC rectangular and T-beams using epoxy adhesives. Laminates are generally preferred to the more rigid plates because they are easier to handle and they do not easily peel off, especially if they are wrapped around the stem of the girder.

Information on the short-term behavior of RC beams strengthened with CFRP laminates is relatively abundant and well documented (Plevris et al 1994 and 1995, Shahawy et al 1996, and Saadatmanesh and Malek 1998). ACI committee 440 is currently developing design guidelines for external strengthening of concrete structures using fiber reinforced polymer systems, and a synthesis of the provisions of the Canadian Highway Bridge Design Code for fiber-reinforced structures has been recently published (Bakht et al 2000).

However, data on long term behavior, especially fatigue response, is still rather limited. Meier et al. (1992) conducted some of the earliest fatigue tests on RC beams strengthened with hybrid glass/carbon laminates. The test results showed that in addition to improving the shortterm behavior of the RC beams, the use of CFRP also improved fatigue behavior. Inoue et al.

(1995) conducted fatigue tests of rectangular RC beams strengthened with CFRP plates. They observed that the behavior of the beams became quite complex leading to several possible secondary modes of failure after the steel reinforcing bars ruptured due to high-cycle fatigue. They concluded that CFRP reinforcement was beneficial to the fatigue performance of the beams, reducing crack width, and improving its distribution prior to failure. Shahawy and Beitelman (1999) conducted accelerated fatigue testing of several RC T-beams strengthened with a varying number of CFRP laminates including a test specimen that was cycled to about half its fatigue life then rehabilitated using CFRP. Test results showed that the application of the CFRP laminates significantly extended the fatigue life of the reinforced concrete beams, including the beam that had accumulated fatigue damage prior to rehabilitation using CFRP. These test results along with other fatigue tests reported by Barnes and Mays (1999) highlight the benefits of using CFRP laminates and plates to rehabilitate deficient reinforced concrete bridge girders.

This paper presents a technique for simulating the accelerated fatigue behavior of reinforced concrete beams strengthened with CFRP. The method proposed in this paper is implemented in a computer program, which accounts for the nonlinear time-dependent response of the composite system. The developed program is used to conduct static and fatigue analyses of reinforced concrete beams strengthened with CFRP laminates tested by Shahawy and Beitelman (1999, 2000) and Barnes and Mayes (1999). Based on the analyses, design considerations are suggested for the repair and/or strengthening of reinforced concrete beams using CFRP laminates.

FIBER SECTION ANALYSIS

The static and fatigue analyses presented in this paper are based on the fiber section technique. The fiber section method is an accurate and practical technique for computing the

moment-curvature response of a reinforced concrete section strengthened with CFRP. As shown in Fig. 1, fiber section analysis of a composite cross section entails discretization of the section into many small layers (fibers) for which the constitutive models are based on uniaxial stressstrain relationships. Each region represents a fiber of material running longitudinally along the member and can be assigned one of several constitutive models representing concrete, CFRP, or reinforcing steel. The main assumptions employed in the fiber section method are:

- Plane sections are considered to remain plane after bending. It is generally accepted that this assumption is reasonable even well into the inelastic range. Measurements of strains along the height show that this assumption is good for beams with either partial or full wrapping (Shahawy and Beitelman 2000 and Inoue et. al 1995)

- Perfect bond is assumed between concrete and other materials (steel reinforcement and CFRP laminates).
- Shear stresses are not accounted for. The fiber section method, as presented in this paper, is therefore limited to long thin members whose behavior is dominated by flexure.

In their discretized form, the cross-sectional forces are determined as stress resultants according to the following equations:

$$P = \sum_{i=1}^{n} S_i A_i \qquad (1)$$

$$M_z \sum_{i=1}^{n} S_i A_i d_i$$

where:

P axial load

M_Z major bending moment

S_i longitudinal stress at centroid of fiber *i*

A_i area of fiber *i*

d_i distance between centroid of fiber *i* and top of section.

n total number of section fibers

The general solution procedure is organized around calculating the moment-curvature response for a fixed value of axial load, P, where, P=0 for the case of pure flexure. The moment curvature response is obtained by incrementally increasing the curvature and solving for the corresponding value of moment. The location of the neutral axis and the fiber strains are a function of the curvature, ϕ , and strain at the extreme top fiber, ε_t, Based on the "plane sections remain plane" assumption, the fiber strains are equal to ε_t, minus the product of the curvature times the orthogonal distance from the centroid of each fiber to the neutral axis (see Fig. 1). The fiber stresses in Eqs. 1 and 2 above are calculated from the fiber strains using appropriate constitutive relationships. For given values of curvature, the top fiber strain is solved for by iteration until the specified value of *P* is reached. Resulting from this process is a set of unique values of moment, M_Z, and curvature, ϕ. The moment-curvature calculations are stopped when a prespecified number of curvature increments are applied. Further details regarding the

application of the fiber section method to composite cross-sections can be found in El-Tawil et al (1995). Once the moment curvature relationship of a cross-section is determined, the load-deflection response of the beam is calculated using the moment area method.

CONSTITUTIVE PROPERTIES OF COMPONENT MATERIALS

The assumed constitutive properties for the component materials are shown in Fig. 2. The stress-strain response of CFRP is assumed to be elastic-perfectly brittle whereas the stress-strain curve for steel is elastic-plastic with a post yield strain hardening of l %. A nonlinear stress-strain relationship is assumed for concrete fibers, which is described next.

Concrete in Compression

The concrete compressive stress-strain curve is taken after Thorenfeldt (1987) and Popovics (1973):

$$f_c = \frac{n f_c^{'} \left(\varepsilon_{cf} / \varepsilon_c^{'} \right)}{n - 1 + \left(\varepsilon_{cf} / \varepsilon_c^{'} \right)^{nk}} \tag{3}$$

Where:

f_c is the concrete stress.

$f_c^{'}$ is the unconfined compressive strength (cylinder strength).

ε_{cf} is the concrete strain.

$\varepsilon_c^{'}$ is the concrete strain at $f_c^{'}$.

$n = 0.8 + f_c^{'} / 17$ ($f_c^{'}$ in MPa units)

$k = (0.67 + f_c^{'}/62) > 1$ for $(\varepsilon_{cf} / \varepsilon_c^{'}) > 1$. Otherwise $k = 1$. ($f_c^{'}$ in MPa units)

Concrete strength is taken to be 0.85 $f_c^{'}$ instead of $f_c^{'}$ in the analyses. Use of the 0.85 factor is well established in the literature and accounts for (a) basic differences between concrete in a test cylinder versus a reinforced concrete beam due to geometry, steel reinforcement, method of load application, rate of loading, ...etc.; and (b) variations in concrete compaction, water-cement ratio, and curing conditions.

Concrete Cracking

Concrete is assumed to crack when it reaches its tensile strength calculated according to the ACI 318 Code ('Building' 1999). After concrete cracks, tension stiffening occurs in concrete reinforced with CFRP or steel bars. Tension stiffening accounts for load transfer mechanisms that exist between reinforcement (steel bars or CFRP fabric) and surrounding concrete and is generally represented by a gradual degradation in the concrete tensile strength after cracking. It is reasonable to assume that CFRP will generate a greater concrete tension stiffening effect compared to steel bars because it is directly attached to a large concrete surface area. Based on a calibration to beam test results by Shahawy and Beitelman (1999) tension stiffening due to steel bar reinforcement alone is assumed to decrease linearly from 70% of the cracking stress to zero at five times the concrete cracking strain. Tension stiffening due to the presence of both steel and

CFRP combined is assumed to degrade linearly from 70% of the cracking stress to zero at 20 times the concrete cracking strain. These models are shown in Fig. 2b.

TIME-DEPENDENT BEHAVIOR OF COMPONENT MATERIALS

Much work has been done on time-dependent analysis of concrete structures. Bazant (1988) provides a general review of material models and analysis techniques for concrete structures undergoing creep and shrinkage. Rao and Jayaraman (1989) provide a more specific review of models used for the analysis of reinforced and prestressed beams undergoing creep and shrinkage. Among the material models most commonly used are the incremental quasi-elastic stress-strain model and the age-adjusted effective modulus model. In the former, which is more rigorous and accurate, the stress-strain relation for the time step is treated as a quasi-elastic relation, and the structural problem is solved through a sequence of linear steps. In the age-adjusted effective modulus model, the problem is solved in one time step making use of an effective quasi-elastic stress-strain relationship. The model proposed in this paper falls under the first category and is described in the following sections.

Fatigue Response of Concrete

Cyclic loading on concrete produces an effect that is similar to creep, i.e. increase in concrete strain with increasing number of cycles. However, tests have demonstrated that strain accumulation due to a varying load is greater than creep due to a constant load equal to the average of the cyclic load. The difference is dependent on a number of parameters, including stress range, maximum stress, ambient temperature, and humidity (Neville 1996).

Experiments have shown that the stress-strain response of concrete varies with the number of load repetitions ('Considerations' 1974, Neville 1996, Holmen 1982). It starts out with the usual concave shape and quickly transitions to a straight-line then gradually to a characteristic convex shape. Test observations indicate that the closer the concrete is to failure, the more convex its stress-strain response. Since concrete in most structures will typically be subjected to relatively low stress levels under service conditions and will generally not be susceptible to high cycle fatigue failure during the design life, it is reasonable to assume the straight-line constitutive model depicted in Fig. 3 for fatigue calculations. Making use of the straight-line assumption and uniaxial concrete fatigue test data provided by Holmen (1982) and Bennet and Raju (1971) the following concrete material model is proposed. The model is suitable for a loading frequency ranging from 0.83 to 15 Hz ('Considerations' 1974 and Holmen 1982).

Holmen proposed that the total maximum strain at any time and at any number of cycles is the sum of two components. The first component is related to the endurance of the specimen, ε_e, and the second part is a function of the loading time, ε_t, and is essentially a creep strain. In other words:

$$\varepsilon_{max} = \varepsilon_e + \varepsilon_t \qquad 4$$

It was observed from the tests that strain development follows three distinct phases; a rapid increase from 0 to about 10 percent of the total fatigue life, a uniform increase from 10 to about 80 percent, then a rapid increase until failure. Holmen (1982) proposed the following expressions to describe the first and second phases:

For $0 < \frac{N}{N_F} \le 0.1$

$$\varepsilon_{\max} = \frac{1}{E_{\sec}} \left| S_{\max} + 3.18\left(1.13 - S_{\max}\right)\left(\frac{N}{N_F}\right)^{0.5} \right| + 0.413\times10^{-3} S_c^{1.184} \ln\left(t+1\right) \quad (5)$$

For $0.1 < \frac{N}{N_F} \le 0.8$

$$\varepsilon_{\max} = \frac{1.11}{E_{\sec}} \left| 1 + 0.677\left(\frac{N}{N_F}\right) \right| + 0.413\times10^{-3} S_c^{1.184} \ln(t+1) \quad (6)$$

where:

$\varepsilon_{\max}$ maximum total strain

$E_{\sec}$ initial secant modulus = $\frac{S_{\max}}{\varepsilon_0}$

ε_0 maximum total strain in the first load cycle

S_{max} ratio of maximum stress to concrete strength

S_c characteristic stress level = S_m + RMS

S_m mean stress ratio = $\frac{1}{2}$ (S_{min} + S_{max})

S_{min} ratio of minimum stress to concrete strength

N number of load cycles

N_F number of load cycles to failure for a specified probability of failure. For example, for a 50% probability of failure, and for S_{min} =0.05, the number of cycles to failure can be calculated from $\log N_F = 1.839\, S_{\max}^{-3.033}$ (Holmen 1982)

t duration of alternating load in hours

RMS root mean square value = $\sqrt{\frac{1}{T_0}\int_0^T x^2(t)dt}$

x(t) stress as a function of time, *t*

T_0 total time, i.e. duration of loading.

According to Holmen (1982), the RMS value for sinusoidal loading is given by

$$RMS = \frac{1}{2\sqrt{2}}(S_{min} + S_{max}) \qquad 7$$

Based on calibration to test results in Bennet and Raju (1971) and Holmen (1982), the following equation is proposed for the effective modulus of elasticity.

$$E_N = \left(1 - 0.33\frac{N}{N_F}\right)E_{\sec} \qquad 8$$

where:

E_N is the effective concrete modulus of elasticity at N cycles.

Knowing S_{max}, ε_{max}, and E_N defined using Equations 4 through 8, a relationship can be constructed that represents the compressive stress-strain response of concrete as a function of the applied stresses and number of load cycles. Concrete under tension is assumed to have no significant tensile strength during cyclic fatigue calculations. The proposed stress-strain curve is shown in Fig. 3.

Additional Model Assumptions

The proposed concrete fatigue model makes use of a number of additional assumptions. It is assumed that the concrete water content and ambient temperature associated with a particular specimen to be analyzed are comparable to those in Holmen's tests. It is further assumed that the model, which is calibrated to uniaxial data, is applicable to concrete subject to a strain gradient. Test results indicate that a strain gradient can influence the fatigue behavior of concrete, typically resulting in a slower rate of strength degradation with increasing number of cycles ('Considerations' 1974). However, fatigue tests on eccentrically loaded concrete are limited, and there is insufficient information to calibrate the proposed model to account for this effect. It is also assumed that the shrinkage strain is negligible compared to the cyclic fatigue strain. This is justifiable since the proposed model is mostly useful for analyzing beams subjected to accelerated fatigue loading, in which the duration of the test is rather short - two to three weeks.

Fatigue Response of Steel, CFRP, and Epoxy

Experimental results presented in Barsom and Rolfe (1987) suggest that the modulus of elasticity for steel remains unchanged until just before failure by high cycle fatigue. Furthermore, test data in Hull (1981) and Hollaway and Leeming (1999) suggests that the behavior of CFRP is virtually unaffected by fatigue loading. Hence, the modulus of elasticity for both steel and CFRP is assumed to remain unchanged during cyclic loading. Furthermore, the epoxy between the CFRP laminates and concrete is assumed to be rigid and unaffected by cyclic loading. This is a reasonable assumption for beams in which failure initiates in the high moment zone, where shear stresses in the epoxy are low.

FATIGUE CALCULATIONS

As fatigue loading progresses, the stress-strain response of each concrete fiber changes as a function of the number of cycles and maximum and minimum stresses generated within the fiber (see Fig. 3). To simulate the fatigue behavior of a cross-section, the analysis is conducted in increments of cycles, say 10,000 cycles each, and the concrete constitutive model is updated at the end of each block of cycles. It is assumed that the concrete model does not change within each set of cycles.

The maximum and minimum stresses in each fiber can change considerably during the analysis, affecting the cyclic creep strain calculation and the corresponding constitutive relationship. As shown in Figure 3, the cyclic creep strain is equal to ε_{max} minus the elastic component of strain. The change in stress levels during the analysis is taken into account using the principle of superposition. The principle of superposition states that the creep strain response

(in this case cyclic creep strain) of concrete to a sum of two stress histories is the sum of the responses to each of them taken separately. The superposition principle is generally deemed reasonably accurate when applied to concrete within the service stress range (Bazant 1988).

A fatigue simulation starts by conducting a monotonic moment-curvature analysis of the beam cross-section. The purpose of this step of the analysis is to obtain the maximum and minimum stresses in each fiber corresponding to the application of the maximum and minimum moments. These stresses are utilized to construct concrete constitutive models for each individual fiber using Equations 4 through 8. The developed constitutive model for each fiber is assumed to represent fiber behavior at the beginning and during the following (second) block of cycles. Using the constructed constitutive models, a second monotonic analysis is conducted to calculate the moment-curvature response of the section during the second block of cycles. The maximum and minimum stresses calculated from the second monotonic analysis are used as input stresses for the third set of cycles and new stress-strain curves for each fiber are constructed using Eqs. 4 through 8. The process described above is repeated to compute the response of the cross-section for any number of cycles.

The sequence of steps taken by the program to update the cyclic creep strains can be better understood by examining Fig. 4. At the beginning of the first block of 10,000 cycles, the maximum stress in a particular fiber is say, S_{max1} and the cyclic creep strain is zero. At the beginning of the of the second block of cycles, the maximum stress in the same fiber drops to S_{max2} by an amount ΔS_{21}, and the accumulated cyclic creep strain is ε_{cr1}. At the beginning of the third block of cycles, the maximum stress in the fiber drops to S_{max3} by an amount ΔS_{32} and the accumulated cyclic creep strain is $\varepsilon_{crs} - \Delta\varepsilon_{21}$. The quantity, ε_{21}, is calculated as if the stress, S_{max1},

had been acting for 20,000 cycles. According to the superposition principle, the correction DE21 is algebraically added (in this case subtracted because the stress is dropping) and represents the accumulated creep strain due to ΔS_{21} acting for 10,000 cycles, between the ends of cycle increments 1 and 2. The process can then be repeated for subsequent blocks of cycles. The solution method requires some bookkeeping to keep track of corrections, which increase with the number of cycle increments. Nevertheless, programming the process is quite straightforward.

The above described procedure has been implemented in a computer program T-DACS (Time-Dependent Analysis of Composite Sections) and is verified and exercised by comparing analytical results to test data in Shahawy and Beitelman (1999, 2000) and Barnes and Mays (1999). Numerical studies using T-DACS show that accuracy of the analysis does not increase significantly when the number of cycles per step is less than 10,000, and so the following calculations are conducted using 10,000 cycles per step.

ANALYSIS OF SHAHAWY AND BEITLEMAN'S (1999, 2000) SPECIMENS

Tests of reinforced concrete beams strengthened with CFRP laminates were conducted at the FDOT Structures Lab (Shahawy and Beitelman 1999 and 2000). The four-point flexural tests were designed to study the effect of concrete strength and number of laminates on the fatigue behavior of reinforced concrete beams rehabilitated with CFRP laminates. The test program consisted of both static and fatigue tests of 23 specimens. Figures 5 and 6 show the test setup and cross-section details. Further details may be found in Shahawy and Beitelman (1999 and 2000).

Two series of specimens were tested. The first series (Shahawy and Beitelman 1999) was subjected to fairly low moments ranging from 44 to 89 kN-m which correspond to 25 to 50% of

the flexural capacity of the reinforced-concrete cross section. The second series (Shahawy and Beitelman 2000) was subjected to moments that were somewhat higher ranging from 44 to 132 kN-m which correspond to 25 to 75% of the flexural capacity of the reinforced concrete cross section. The stirrups in the first series were tack welded to the main bar reinforcement, which caused the bar reinforcement in the control beam (without CFRP strengthening) to fracture early on in the cyclic load history. The beams in the second series did not have any tack welding.

The CFRP fabric utilized in the tests was composed of unidirectional dry carbon material formed by weaving individual yarns into a fabric. The yarn density is 2.5/cm x 2/cm and each yarn has a cross-sectional area of pure carbon of 0.45 mm^2. The fibers have a manufacturer's reported ultimate strength of 3654-MPa, an elastic modulus of 210-GPa, and an ultimate strain of 0.014. The strength of the composite laminates was calculated to be 2137 MPa by assuming the strength of the carbon fibers to follow a Weibull statistical distribution as described in Okeil et al. (2000). The yield stress for steel was measured to be f_y=434-MPa.

All specimens subjected to monotonic loading failed by fracture of the CFRP laminates in the high moment zone. Specimens subjected to cyclic loads failed in the high moment region by high-cycle fatigue fracture of the main steel reinforcement.

Monotonic Analyses

A series of monotonic fiber element analyses were carried out. The analyses were conducted for the control beam and beams with 1, 2, 3, and 4 CFRP laminates. Analytically calculated moment vs. curvature results for all cross-sections are plotted in Fig. 7 along with the measured

response. It is clear from the figures that the analytical response correlates well with the experimental data at all stages of behavior up to failure.

Examination of Fig. 7 reveals that the moment-curvature response of the strengthened beams drops suddenly when the moment capacity is attained. The drop corresponds to rupture of bottommost layer of CFRP laminates and becomes larger as the number of layers increase. Immediately after the sudden drop in moment-curvature response, there is a more gradual reduction in strength. This portion of the response corresponds to the vertical propagation of rupture of the CFRP laminates up the sides of the web. The curve is jagged because of the relatively coarse fiber discretization. Each small drop in the descending curve corresponds to a fiber fracturing. The curve becomes smoother as the discretization becomes finer.

Cyclic Analyses

The measured and computed mid-span deflections for beams with 2 and 3 CFRP layers are plotted versus the number of cycles in Fig. 8. In the figure, beams in which only the end designation is different (i.e. A or B) are identical in all respects, and were tested in the same manner (Shahawy and Beitelman 1999 and 2000). It is clear from the figure that the computed response compares favorably to the measured deflections, with the exception of Beam F-3L5-A, which suffered a sudden jump in deflection at about 1.7 million cycles. This sudden increase in deflection is attributed to an early fatigue fracture of one of the reinforcing bars. However, in spite of the loss of one of the bars, the beam was still capable of sustaining the applied load for over 3 million cycles.

The internal redistribution of stresses due to cyclic creep within a cross section is illustrated in Fig. 9. The calculated stress in the topmost concrete fiber of the specimen with 2 CFRP layers is plotted versus the number of cycles in Fig. 9(a). As is typical of creep behavior, the concrete stress drops rapidly during the initial loading cycles then flattens out. The stress in the steel exhibits an opposite trend, rising rapidly then slowing considerably as can be seen in Fig. 9(b). The overall rise in steel stress is mild, increasing from 324 MPa to 340 MPa - a less than 5% increase. The stress in the carbon fiber also increased by about the same percentage. The increase in steel and CFRP stresses in all the other specimens was also less than 5%.

Fatigue Life of Specimens

To further study the fatigue response of Shahawy and Beitelman's beams, the S_r-N curves are plotted for both unwelded and tack-welded specimens. It was observed from the analyses that even though the steel stress increases mildly as the number of applied cycles increases, the stress range, which is the difference between maximum and minimum stresses in the reinforcement, was essentially unchanged. The calculated stress range is plotted versus the number of cycles to failure in Figure 10.

Corley et al (1971) conducted an extensive experimental investigation to determine the fatigue strength of deformed reinforcing bars. The experimental program covered many variables and involved hundreds of tests. The dotted lines plotted in Figure 10 bound the data presented in Corley et al (1971). It is clear from the figure that the unwelded specimens fall within these bounds, while the tack-welded beams falls well below the lower bound for Corley's data. This is expected since tack-welding causes stress-risers, which significantly reduce fatigue life. An

obvious conclusion that can be drawn from Figure 10 is that increasing the number of CFRP layers reduces the steel stress range leading to an enhancement in fatigue life.

ANALYSIS OF BARNES AND MAYS' (1999) SPECIMENS

Further verification of the program is sought by comparing analysis results to test data in Barnes and Mays (1999) who also conducted accelerated fatigue tests of a series of reinforced concrete beams. The 2300-mm long beams, which had a rectangular cross-section (130-mm wide, and 230-mm deep), were subjected to a cyclic load in four-point bending at a frequency of 1Hz. Unidirectional CFRP (Toray T300) plates were bonded to the bottom surface of the beam. Figures 11 (a) and 11 (b) show the calculated and measured mid-span deflection plotted versus the number of cycles for the control beam (Beam 2) and another beam reinforced with a CFRP plate (Beam 4), respectively. The upper two curves in either figure correspond to the deflection at the maximum applied load, whereas the lower two curves correspond to the lower load. Once again, the analysis results compare favorably to the test results.

DESIGN CONSIDERATIONS

There is growing consensus among structural engineers that CFRP laminates are suitable for repairing or strengthening reinforced concrete beams subjected to flexure. An example of a repair situation is when a structure suffers damage such as corrosion of a few steel reinforcing bars or prestressing strands and needs to be returned to its original strength. The latter case is normally encountered when an existing structure needs to be strengthened to meet increased strength demands, e.g. due to heavier traffic loads. In either case, the CFRP is usually attached to the structure while still subjected to dead load. Under such conditions, the steel bars are already

significantly stressed. Since CFRP ruptures at a strain that is considerably higher than the steel yield strain, it is conceivable that steel reinforcement in a flexurally repaired/strengthened beam may yield under service conditions, i.e. application of the dead plus full live load. Steel yield under service conditions must be avoided because it can cause a reduction in the effective stiffness of the member and can result in excessive permanent deformations, both of which lead to severe serviceability problems.

This situation can be easily remedied during design of the rehabilitation scheme by limiting the steel stress (σ_s) under service conditions such that

$$\sigma_s < \alpha\beta f_y \qquad 9$$

where both α and β are factors that are less than 1.0. The reduction factor a takes into consideration the increase in steel stress, which results from the time-dependent redistribution of stresses due creep, shrinkage, and cyclic fatigue. Analyses by Moustafa (1986) and Rao and Jayaraman (1989) of rectangular reinforced concrete sections show that reinforcing steel stresses increase by less than 3.1% as a result of creep and shrinkage. Cyclic fatigue analyses presented in this paper of the test specimens of Shahawy and Beitelman (1999, 2000) and Barnes and Mays (2000) show that the beams suffer less than 5% increase in steel stresses until failure. In general, the steel stress increase is dependent upon the time elapsed, number of cycles the bridge has been subjected to prior to rehabilitation, ambient temperature and humidity conditions, etc. and therefore it is difficult to draw a firm conclusion from these numbers regarding a precise and conservative value for a. Until further research is conducted, it is recommended that the factor a be taken as 0.90.

The reduction factor β accounts for the possibility that the tensile strength of steel is less than the assumed nominal stress. A review of the literature shows that steel reinforcement strength is normally distributed, has a strength bias of 1.125 (i.e. mean strength is higher than the nominal design value by 12.5%), and a coefficient of variation, COV (ratio of standard deviation to mean) of 10% (Plevris et al. 1995). For a designer to have 95% confidence that the steel yield stress will not fall below the nominal strength, the design stress, f_{des} , should be restricted to

$$f_{des} = \text{mean} - 1.645 \times \text{standard deviation} \quad (10)$$

Using the values of the bias and COV listed above, it turns out that the reduction factor β should be 0.96 ($1.125\, f_y$ - 1.645 x $0.10\, f_y = 0.961\, f_y$).

Substituting the recommended values of a and P into Eq. 9 results in $\sigma_s < 0.86$ - say $\sigma_s < 0.85\, f_y$. In other words, a designer involved in the design of a rehabilitation scheme should limit the steel stress under service conditions to 85% of the yield strength.

CONCLUSIONS

A model for simulating the static and accelerated fatigue behavior of reinforced concrete beams strengthened with CFRP is presented. The model is based on the fiber section technique and accounts for the nonlinear time-dependent behavior of concrete, steel yielding, and rupture of CFRP laminates. The cyclic fatigue response of concrete is based upon test data in Holmen (1982) and Bennet and Raju (1971). The model is implemented in a computer program and is

verified and exercised by comparing analytical results to data from two experimental investigations.

A study of the internal stresses obtained from the model showed that cyclic fatigue leads to an internal redistribution of stresses similar to that obtained under static creep. The analyses show that the steel reinforcement stress in the specimens of Shahawy and Beitelman (1999, 2000) and Barnes and Mays (2000) increased by less than 5% during the fatigue life of the test beams. To account for the increase in steel stresses due to cyclic fatigue as well as shrinkage, creep under dead loads and the variability in reinforcing steel strength, it is recommended that the service steel stress be limited such that $\sigma_s < 0.85\, f_y$ for repair and/or strengthening of reinforced concrete girders using CFRP laminates. The 0.85 factor is affected by a variety of parameters and further research is needed to refine it.

ACKNOWLEDGEMENT

The authors gratefully acknowledge the financial support provided in part by the Florida Department of Transportation (Contract # BC-190) and the Department of Civil and Environmental Engineering at the University of Central Florida. The contribution of Tom Beitelman to this research is greatly appreciated.

REFERENCES

Bakht, B., Al-Bazi, G., Banthia, N., Cheung, M., Erki, M., Faoro, M., Machida, A., Mufti, A., Neale, K., and Tadros, G. (2000) "Canadian Bridge Design Code Provisions for Fiber-Reinforced Structures, *"Journal of Composites for Construction,* ASCE, 4(1), pp. 3-15.

Barnes, R. A. and Mayes, G. C. (1999), "Fatigue Performance of Concrete Beams Strengthened with CFRP Plates," *Journal of Composites for Construction,* ASCE, 3(2), pp. 63-72.

Barsom, J. M. and Rolfe. S. T. (1987), *Fracture and Fatigue Control in Structures,* PrenticeHall, Englewood Cliffs, NJ.

Bazant, Z. P. (1988), *Mathematical Modeling of Creep and Shrinkage of Concrete,* Wiley Series in Numerical Modeling in Engineering, John Wiley and Sons, New York.

Bennet, E. W. and Raju, N. K. (1971), "Cumulative Fatigue Damage of Plain Concrete in Compression," Structure, Solid Mechanics and Engineering Design, pp. 1089-1102, Wiley-Interscience, London.

"Building Code Requirements for Structural Concrete." (1999). ACI 318-99, American Concrete Institute, Detroit, Michigan.

"Considerations for Design of Concrete Structures Subjected to Fatigue Loading." (1974). ACI Report 215-74, American Concrete Institute, Detroit, Michigan.

Corley, W. G., Hanson, J. M., and Helgason, T. (1978), "Design of Reinforced Concrete for Fatigue," *Journal of the Structural Division,* ASCE, 104(6), pp. 921- 932.

El-Tawil, S., Sanz-Picon, C. F., and Deierlein, G. G. (1995), "Evaluation of ACI-318 and AISC (LRFD) Strength Provisions for Composite Columns," *Journal for Constructional Steel Research,* Elsevier Applied Science, Essex, England, 34(1), pp. 103-126.

Holmen, J. O. (1982), "Fatigue of Concrete by Constant and Variable Amplitude Loading," ACI Special Publication, *Fatigue of Concrete Structures, SP* 75-4, pp. 71-110, American Concrete Institute, Detroit Michigan.

Holloway L.C. and Leeming M.B. (1999), *Strengthening of Reinforced Concrete Structures: Using Externally-bonded FRP Composites in Structural and Civil Engineering, CRC* Press, Boca Raton Boston New York, Washington, D.C.

Hull, D. (1981), *An Introduction to Composite Materials,* Cambridge Solid State Science Series, Cambridge University Press, London, England.

Inoue, S., Nishibayashi, S., Kuroda, T., and Omata, F. (1995), "Fatigue Strength and Deformation Characteristics of Reinforced Concrete Beams Strengthened with Carbon FiberReinforced Plastic Plates," *Transactions of the Japan Concrete Institute,* Vol. 17, pp. 149*156 (in English).*

Meier, U., Deuring, M., Meier, H., and Schwegler, G. (1992), "Strengthening of Structures with CFRP Laminates: Research and Applications in Switzerland," *Advanced Composite Materials in Bridges and Structures,* K. W. Neale and P. Labossiere, Editors, Canadian Society for Civil Engineers.

Moustafa, S. E. (1986), "Nonlinear Analysis of Reinforced and Prestressed Concrete Members," *Prestressed Concrete Institute Journal, 31(5), pp.* 126-147.

Neville, A. M. (1996), *Properties of Concrete,* 4th Edition, J. Wiley, NY, New York.

Okeil, A.M., El-Tawil, S., and Shahawy, M. (2000), "Short-Term Tensile Strength Of CFRP Laminates For Flexural Strengthening Of Concrete Girders," *Accepted for publication in ACI Structural Journal.*

Plevris, N., Triantafillou, T.C., and Venesiano, D. (1995). 'Reliability of RC Members Strengthened with CFRP Laminates," *Journal of Structural Engineering,* ASCE, 121(7), 1037-1044.

Plevris, N., Triantafillou, T. C. (1994), "Time-Dependent Behavior of RC Members Strengthened with FRP Laminates," *Journal of Structural Engineering,* ASCE, 120(3), pp. 1016-1042

Popovics, S. (1970), "A Review of Stress-Strain Relationships for Concrete," ACI *Structural Journal,* 67(3), pp. 243-248.

Rao, A. S. P. and Jayaraman, R. (1989), " Creep and shrinkage analysis of partially prestressed concrete members," *Journal of Structural Engineering,* ASCE, 115(5), pp. 1169-1189

Saadatmanesh, H. and Malek, A. M. (1998), "Design Guidelines for Flexural Strengthening of RC Beams with FRP Plates," *Journal of Composites for Construction,* ASCE, 2(4), pp. 158-164.

Shahawy, M. and Beitelman, T. E. (2000), *Static and Fatigue Performance of RC Beams Strengthened with CFRP Laminates,* Report, Structural Research Center, Florida Department of Transportation, 2007 East Dirac Drive, Tallahassee, Florida, FL 32310.

Shahawy, M. and Beitelman, T. E. (1999), " Static and Fatigue Performance of RC Beams Strengthened with CFRP Laminates." *Journal of Structural Engineering,* ASCE, 125(6), pp. 613-621

Shahawy, M. A., Arockiasamy, M., Beitelman, T., and Sowrirajan, R. (1996), "Reinforced Concrete Rectangular Beams Strengthened with CFRP Laminates," *Composites, Part B,* 27B, pp. 225-233.

Thorenfeldt, E. Tomaszewicz, A., and Jensen, J. J. (1987), "Mechanical Properties of High Strength Concrete and Application in Design," *Proceedings of the Symposium " Utilization of High Strength Concrete, "* Stavanger, Norway, June 1987, Tapir, Trondheim, pp. 149-159,

LIST OF FIGURES

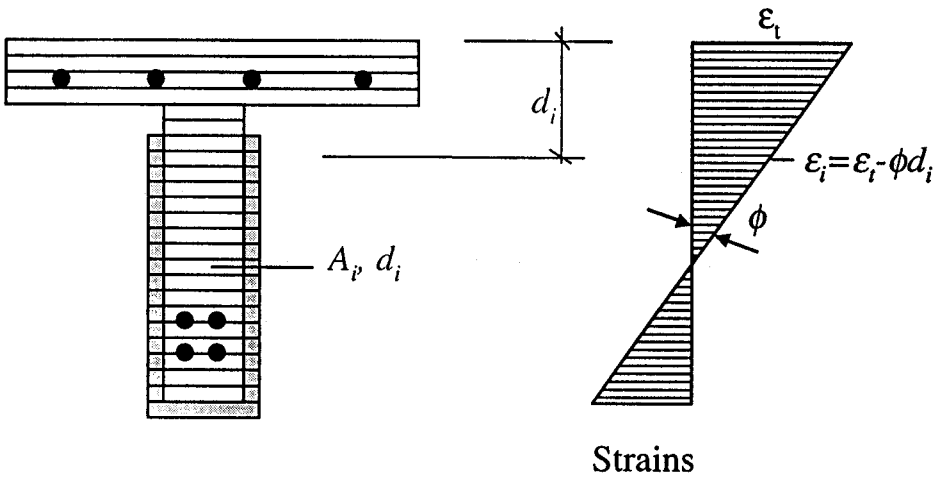

FIGURE I

Fiber section discretization of a reinforced concrete section strengthened with CFRP laminates.

CAN BE REDUCED TO (/8 OF A PAGE

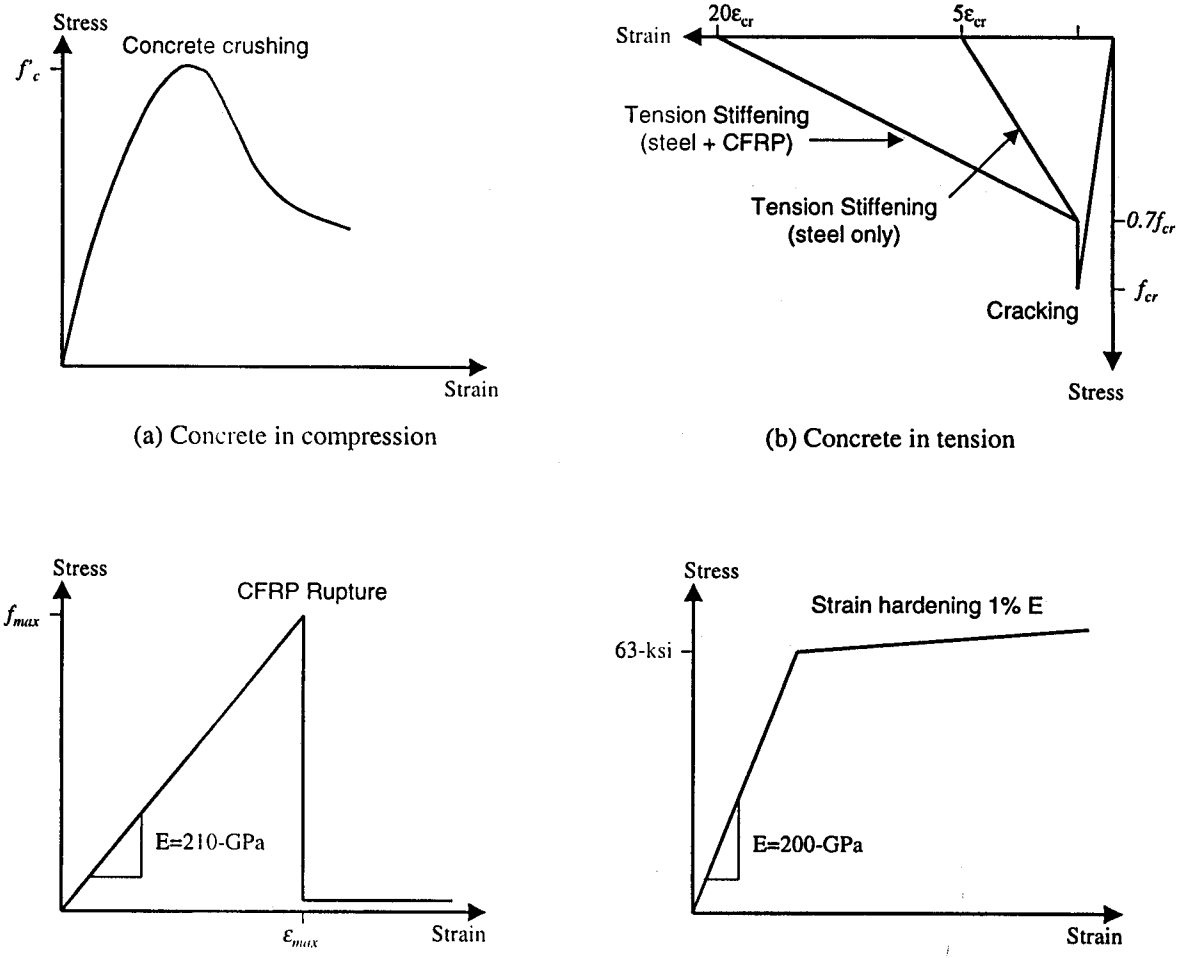

FIGURE 2

Monotonic constitutive models for component materials

CAN BE REDUCED TO 1/4 OF A PAGE

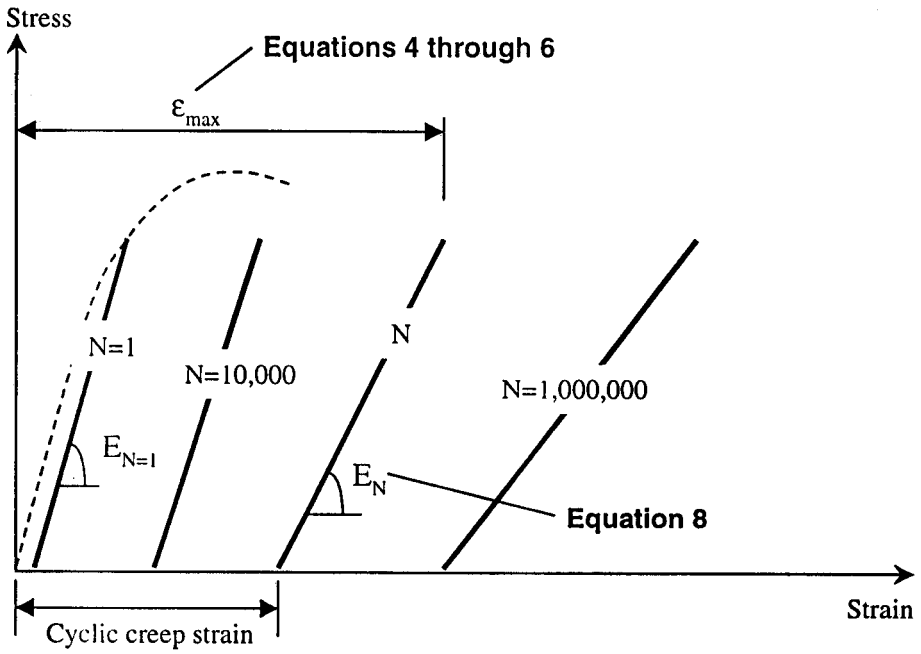

FIGURE 30

Proposed constitutive model for concrete subjected to fatigue loading.

CAN BE REDUCED TO 1/8 OF A PAGE

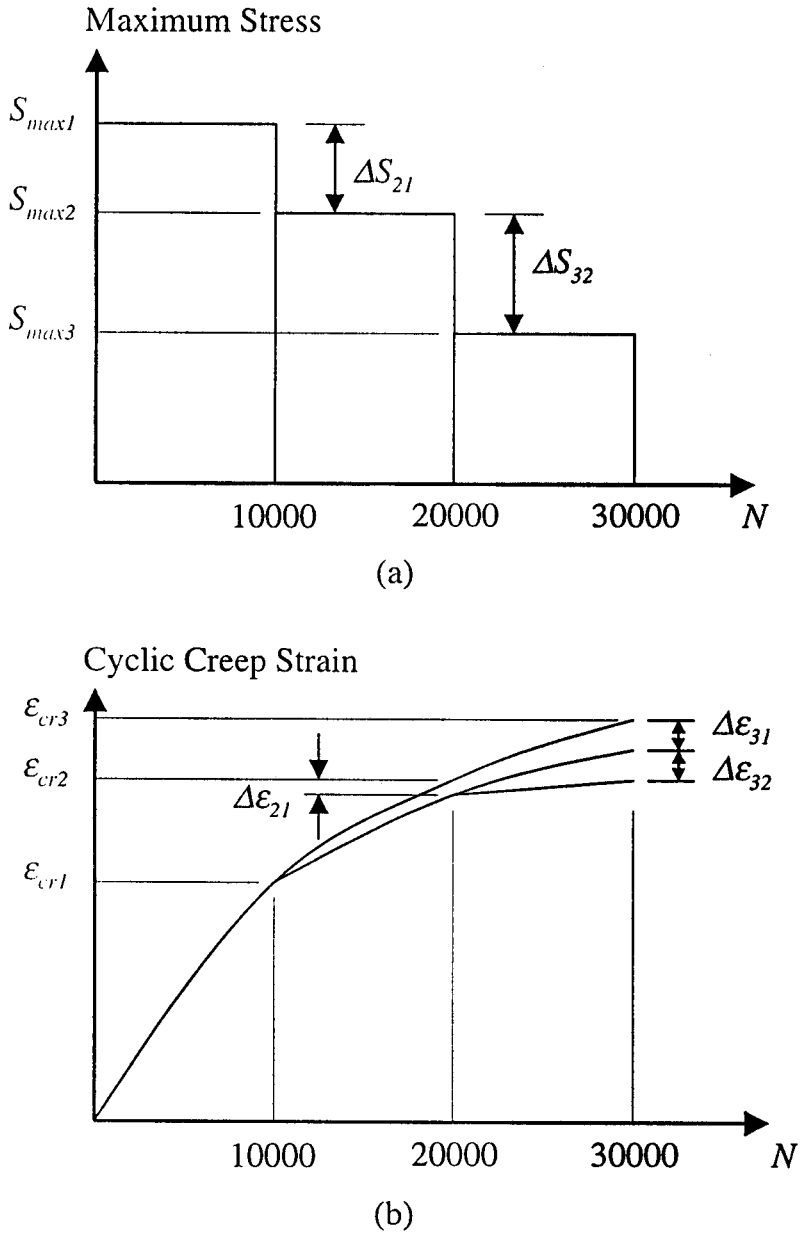

FIGURE 31

Principle of superposition for cyclic creep strain calculations

CAN BE REDUCED TO 1/4 OF A PAGE

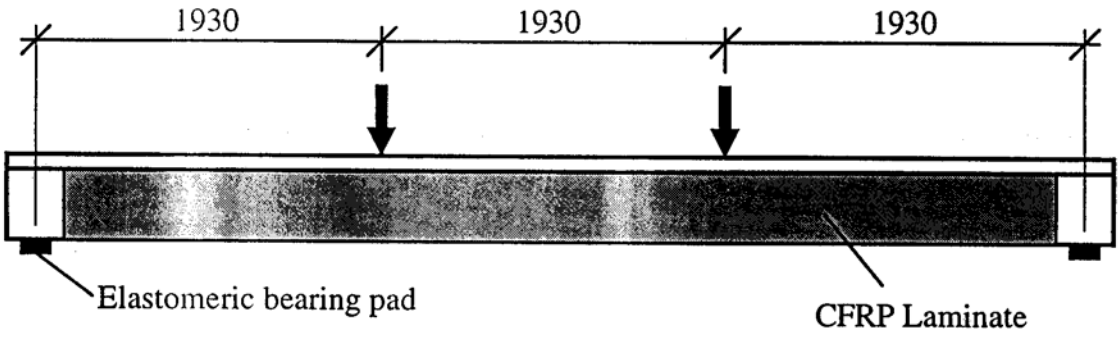

FIGURE 32

Loading setup for MOT girders (dimensions in mm)

CAN BE REDUCED TO 1/4 OF A PAGE

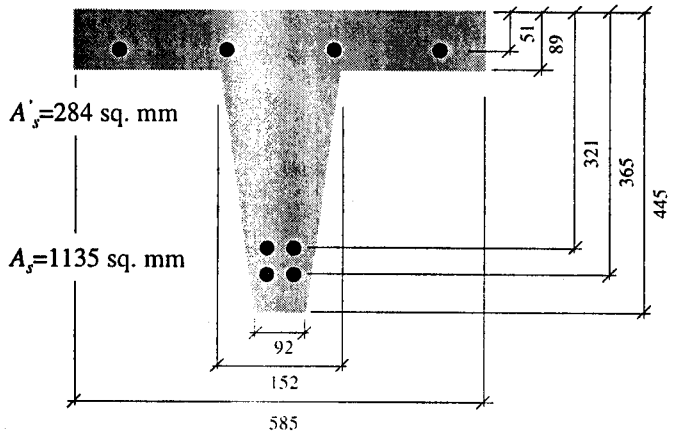

(a) Reinforced concrete section

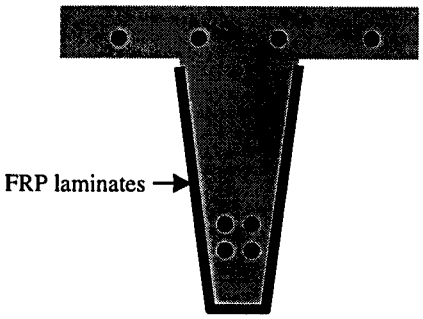

(b) FRP reinforced section

FIGURE 6

Cross-section details (dimensions in mm)

CAN BE REDUCED TO 1/4 OF A PAGE

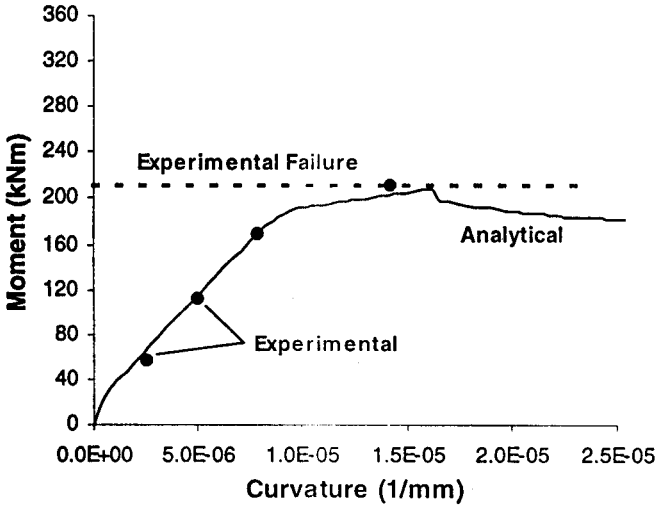

(a) W-1L-5

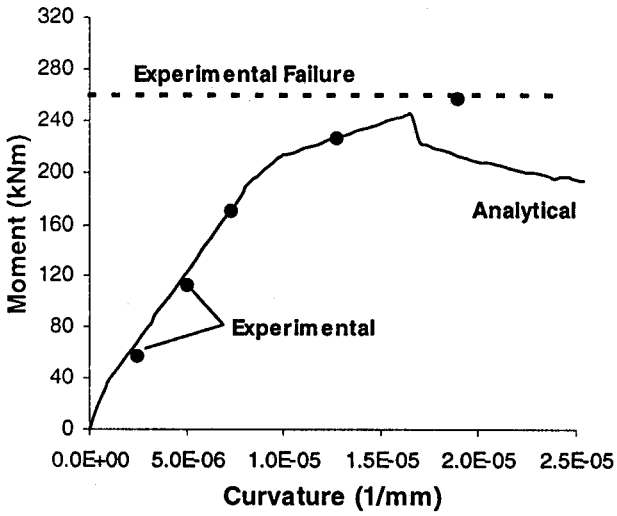

(a) W-2L-5

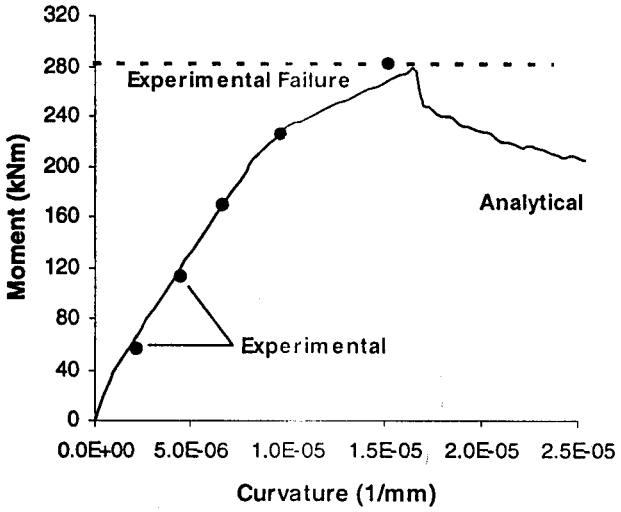

(a) W-3L-5

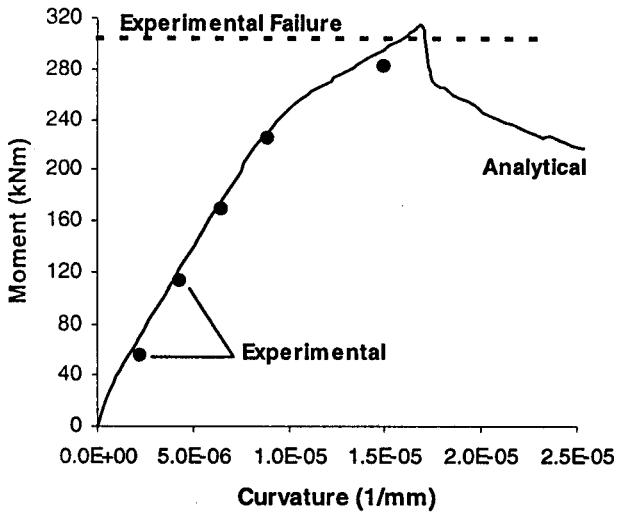

(a) W-4L-5

FIGURE 34

Analytical versus experimental monotonic moment-curvature response

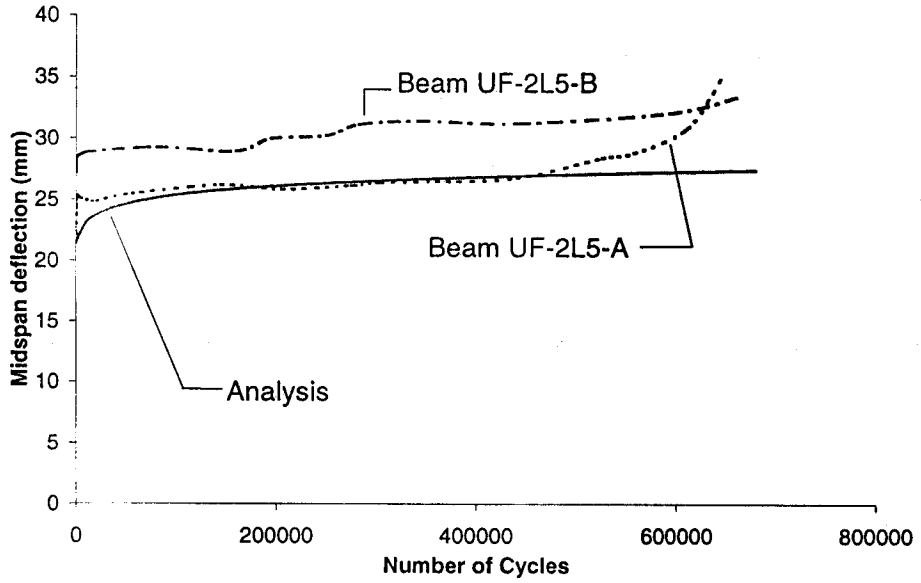

(a)

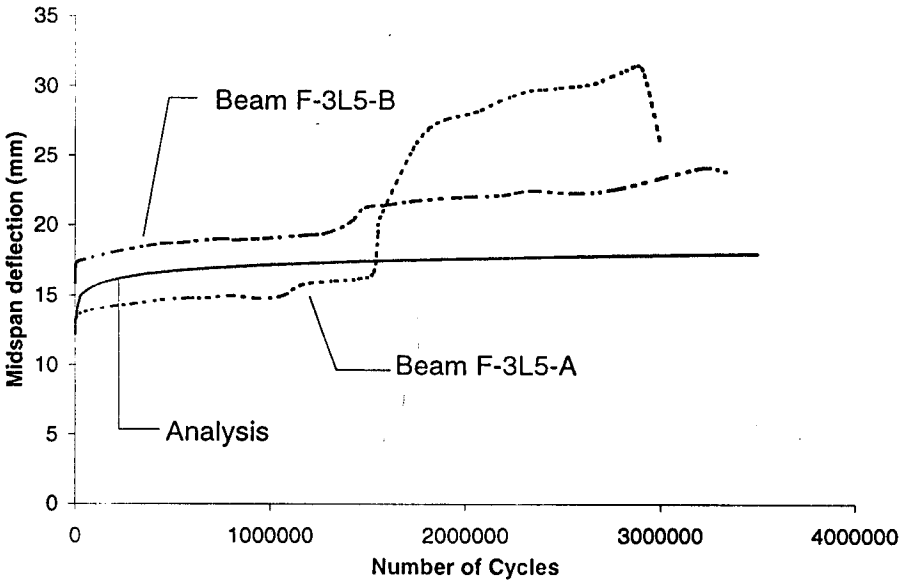

(b)

FIGURE 35

Calculated versus experimental mid-span deflection for (a) beams with 2 CFRP layers (Shahawy and Beitelman 2000) and (b) beams with 3 CFRP layers (Shahawy and Beitelman 1999)

CAN BE REDUCED TO 1/3 OF A PAGE

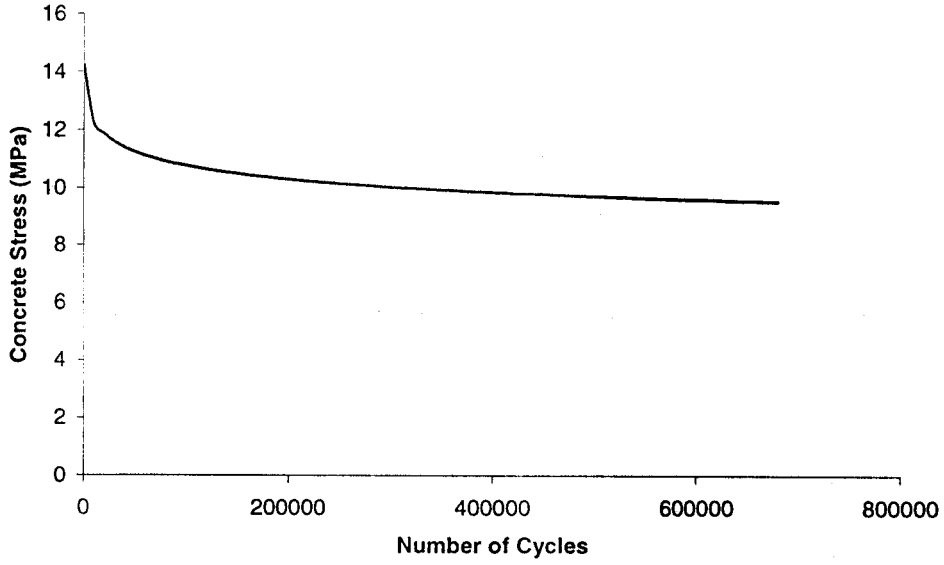

(a)

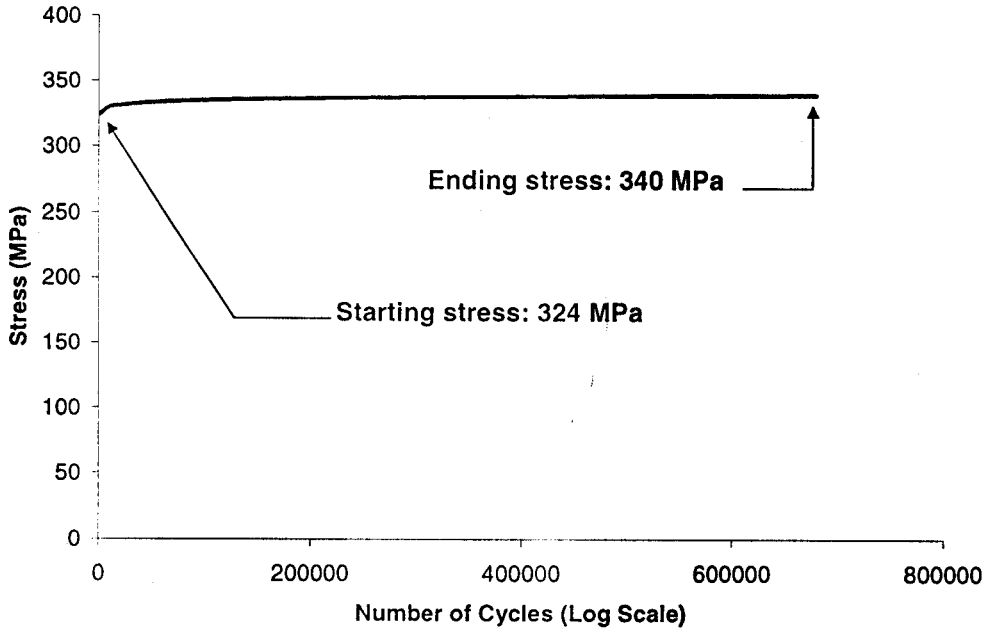

(b)

FIGURE 36

Calculated stresses in (a) top concrete fiber and (b) bottom steel layer versus number of cycles for beam with 2 CFRP layers

CAN BE REDUCED TO 1/3 OF A PAGE

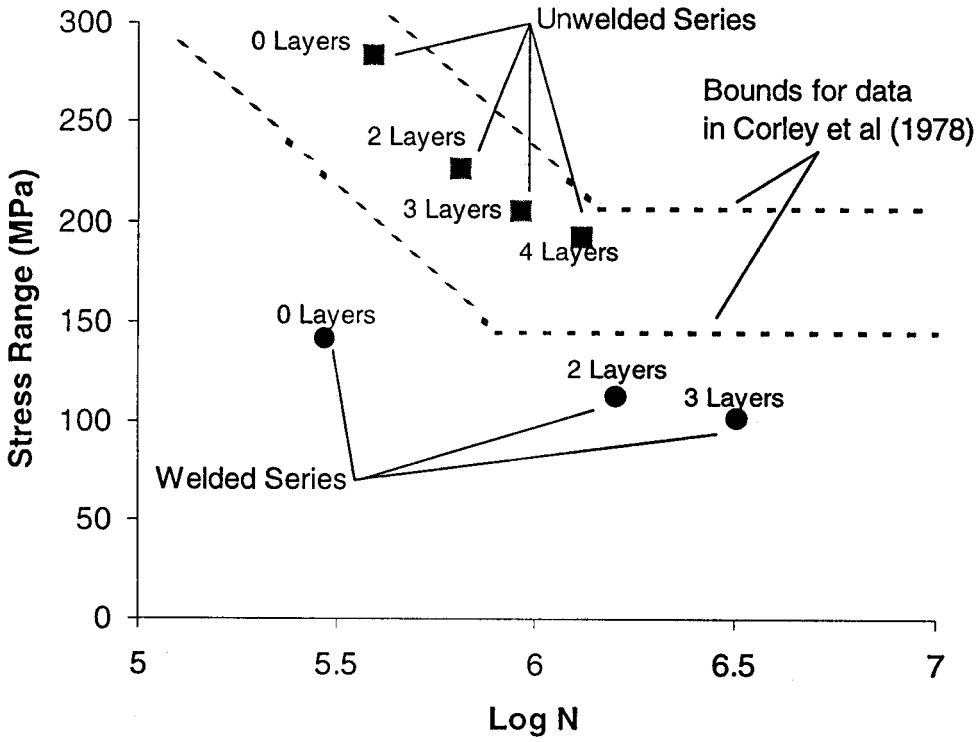

FIGURE 37

S_r-N Curve for Shahawy and Beitelman's (1999, 2000) fatigue tests

CAN BE REDUCED TO 1/4 OF A PAGE

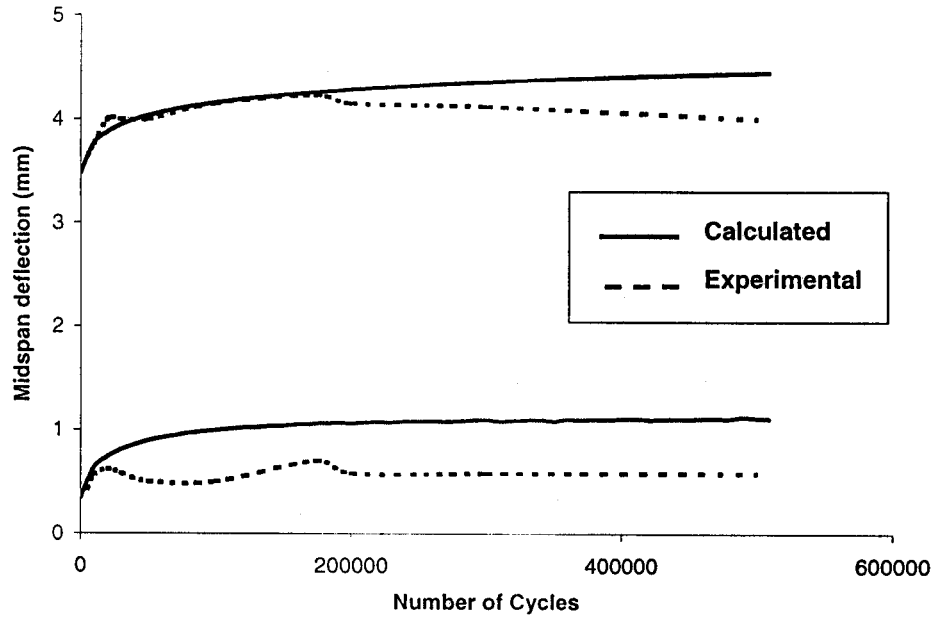

(a)

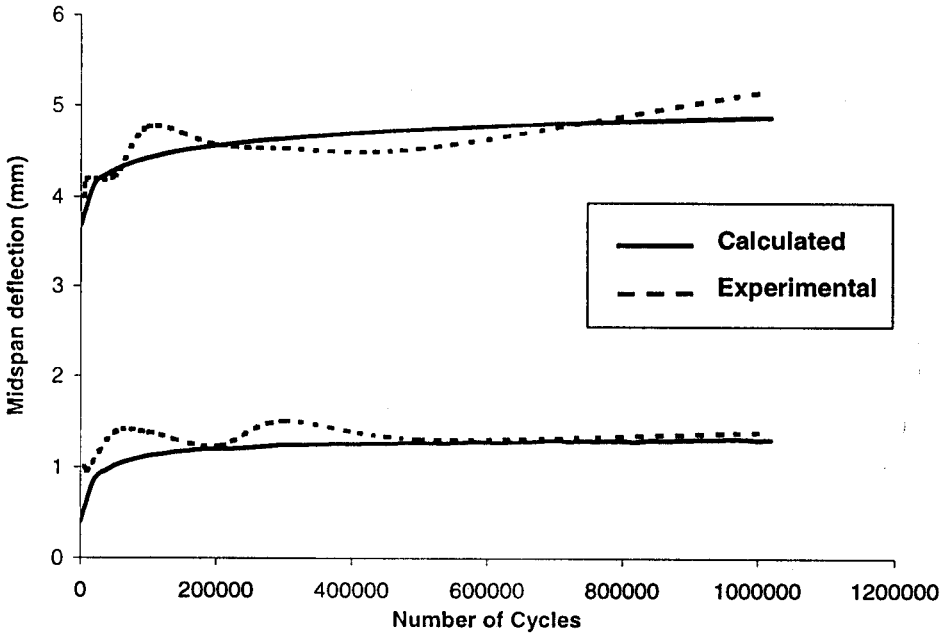

(b)

FIGURE 38

Calculated versus experimental mid-span deflection for (a) Beam 2 and (b) Beam 4 (Barnes and Mays (1999).

KeyWORDS

Accelerated

Cyclic

Fatigue

Concrete

Carbon fiber

CFRP

Fiber section